Simulation and Test Study on Direct Force Control for Permanent Magnet Linear Synchronous Motor

Haixing Wang
School of Electrical Engineering and Automation, Henan Polytechnic University, Jiaozuo, China
Email: wanghaixing@hpu.edu.cn

Haichao Feng[1], Jikai Si[1] and Nan Wu[2]
[1]School of Electrical Engineering and Automation, Henan Polytechnic University, Jiaozuo, China
[2]Wangfang College of Science & Technology, Henan Polytechnic University, Jiaozuo, China
Email: fhc@hpu.edu.cn, sijikai@hpu.edu.cn, rainwn@hpu.edu.cn

***Abstract*—Permanent magnet linear synchronous motor (PMLSM), which has the advantages of simple structure, small volume, high force, is a research focus and difficulties because of the thrust ripple and control problems for PMLSM. In this paper, in order to reduce thrust ripple and improve system control performance, the space voltage vector pulse width modulation technology (SVPWM) was introduced into the directing force control (DFC) strategy of PMLSM. In the running process, the temperature of PMLSM will rise, which changes the resistance of the primary winding. Full consideration of the change of the resistance in the motor running process, the error between the flux observed value and the actual value was analyzed. And then a new flux dynamic compensation algorithm based on flux dynamic compensation was proposed. The novel dynamic compensator was built to improve the observation accuracy of the primary flux, which solved effectively the wrong voltage vector choice and the system control performance failure due to the error of the primary flux. The Simulation and test results show that the PMLSM DFC based on SVPWM and the flux dynamic compensation has better control performance.**

***Index Terms*—permanent magnet linear synchronous motor (PMLSM), SVPWM, dynamic compensation, direct force control (DFC), simulation and test**

I. INTRODUCTION

Linear motor with the advantages of simple structure, low noise, high precision, easy maintenance etc., directly implements linear motion without gears, chains, connecting rod and other intermediate conversion. So, linear motor has been widely used in transportation, industrial equipment, logistics, military, modern high-precision machine tools and other fields, gradually into people's daily life [1~4].

Supported by Henan Province University Key Teacher Foundation (NO. 2010GGJS-230), Doctor Foundation of HPU (NO. 2011065), National Natural Science Foundation of China (NO. 61074095).

Permanent magnet linear synchronous motor (PMLSM) combining the advantages of permanent magnet motor and linear motor. Direct force control (DFC) has advantages such as, clear thought control without complex coordinate transformation, small requirements for the motor parameters, strongly robustness, fast response, and so on. But the thrust ripple and the control effect non-ideal are the existing problems for DFC. How to reduce the speed and thrust fluctuations are the key application problems for the PMLSM DFC. Several factors result in the thrust ripple of PMLSM DFC. The discontinuous space voltage vector switching and the observation errors of primary flux are the important [5~8].

In this paper, focused on the existing thrust ripple of the DFC, the SVPWM will be introduced into the PMLSM DFC. At the same time, full consideration of the motor running process with the rise of temperature, a new flux dynamic compensation algorithm is proposed. The dynamic compensator is built to improve the observation accuracy of the primary flux, which maybe cause the wrong choice for the voltage vector and result in the system control performance deterioration, even failure. The proposed flux dynamic compensator solves effectively the wrong voltage vector choice and the system control performance failure due to the error of the primary flux, improving the control performance.

II. SPACE VOLTAGE VECTOR PULSE WIDTH MODULATION

A. Principle Analysis of SVPWM

Space voltage vector pulse width modulation (SVPWM) technology looks the inverter and motor as a whole. Based on the concept of space vector, three phase power generated circular flux as a reference. Through the switch state's choice of the inverter produced the PWM waveform, the vertex along the circular trajectory in order to direct to control motor flux vector amplitude approximately constant, average speed can be adjusted, achieving the frequency conversion voltage control of the motor.

doi:10.4304/jcp.8.3.733-740

SVPWM divides each sector into a number of corresponding switching period between the cell interval, in which the size of the switching period determined by the switching frequency [9~12].

Each cell interval is composed of six effective space vector and two zero vector, which form different linear combination as the equivalent reference vector u_{ref} to make motor flux track approaching circular. In any short period, the inverter output and the reference voltage u_{ref} output are consistent. As shown in Figure 1, in a calculation period T_p, the voltage vector is assumed in the third sector, and the voltage vector u_{ref} is the linear combination of u_4 and u_6.

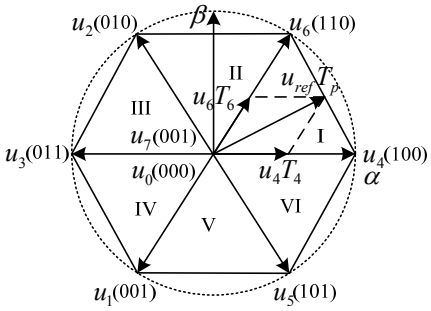

Figure 1. Resolution graph of voltage vector.

If both the role of time equal to zero vectors, according to the total time constant principle gets the action time of two zero vectors. After the action time of each voltage vector determined, then the next is to determine the action order of each voltage vector, which has to follow the principle of switching frequency least. That is from a vector to another vector in the process, only one power device state changes, which can minimize the maximum deviation of each phase current vector. SVPWM has lots of advantages, such as effectively inhibit harmonic component, reduce the current waveform distortion, and greatly improve the utilization of DC voltage, and make the rotating magnetic field closing to circular, so as to achieve higher control performance.

B. SVPWM Simulation

The SVPWM simulation needs the judgment of the sector, the action time calculation, the distribution of the voltage vector, and the decision of the switching vector points, and so on.

It is known that SVPWM can be realized long as the two-dimensional static coordinate component u_α and u_β of the reference voltage vector u_{ref}, and the calculation period of the PWM T_s, where the half of the PWM period is T_p.

So the SVPWM can be realized following the three steps. Firstly, the sector should be determined. Secondary, the synthesis of the action time of two adjacent vectors should be determined. Finally, the switching points of the vector T_{cm1}, T_{cm2}, and T_{cm3} should be calculated.

The simulation model of SVPWM shown in Figure 2, mainly including the module of the judgment of the sector, the module of the X/Y/Z calculation, the module of the action time of T_1 and T_2 calculation, the module of the vector switching point, and the pulse generator module.

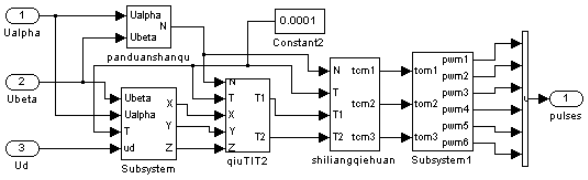

Figure 2. Simulation module of SVPWM.

Simulation of the SVPWM module, the simulation results were shown in the figures from Figure 3 to Figure 6. Figure 3 is the simulation waveform of the sector *N*. Figure 4 shows simulation waveform of the vector action time. Figure 5 is a modulation waveform of the vector switching point T_{cm1}. Figure 6 shows pulse waveform of SVPWM.

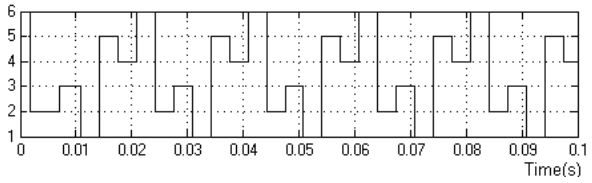

Figure 3. Simulation waveform of sector *N*.

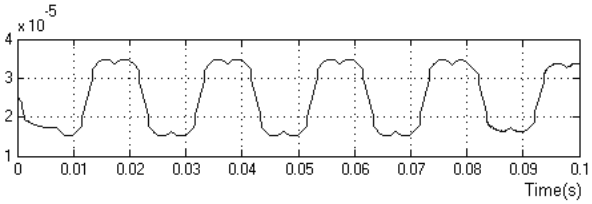

Figure 4. Modulating waveform of T_{cm1}.

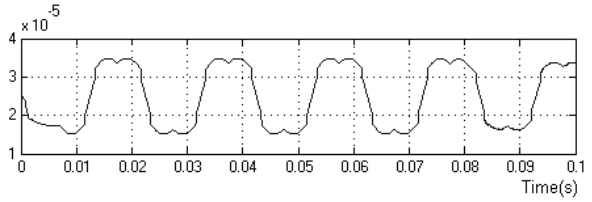

Figure 5. Modulation waveform of T_{cm1}.

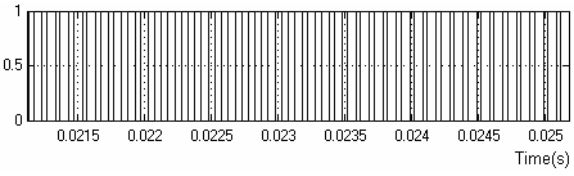

Figure 6. Waveform of SVPWM.

As the Figure 3 shown, the cycle of sector *N* is 2→3→1→5→4→6, and the work order of the corresponding sector is VI→I→II→III→IV→V. It can be seen from the Figure 5, the modulation waveform T_{cmx} (x=1, 2, 3) are three-phase saddle, so it has the advantages to optimize the PWM inverter.

III. Design of Flux Dynamic Compensator

A. Presentation of Questions

In the conventional direct thrust control (DFC), using the voltage model, the primary flux observation equation is described as in (1).

$$\psi_s = \int (u_s - R_s i_s)dt + \psi_{s0} \tag{1}$$

In (1), the primary winding resistance is used as the only motor parameters. Of course, the initial flux will also affect the precision of the flux observation. If the primary resistance remains constant, the observed flux values will be consistent with the actual value. In fact, the resistance will change along with the motor temperature and current frequency. Any change in resistance will bring integration error, flux value doesn't match with the actual value, may lead to the choice of error voltage vector, the system control performance degradation.

Making dR_s as the incremental resistance value, and di_s as the corresponding current increase, the actual value of the primary flux is described as in (2).

$$\psi_s = \int (u_s - (R_s + dR_s)(i_s + di_s))dt + \psi_{s0} \tag{2}$$

At present, many scholars regard the resistance in motor control as a constant value, but only as the current changes, and the resulting primary flux observer is in (3).

$$\begin{aligned} d\psi_s &= \psi_s - \psi_s^* \\ &= \int (u_s - (R_s + dR_s)(i_s + di_s))dt - \int (u_s - R_s(i_s + di_s))dt \\ &= \int dR_s(i_s + di_s)dt \end{aligned} \tag{3}$$

As shown in (3), resistance change is bound to affect flux observer accuracy, which is a non-negligible factor.

Recently, focused on the problem of the resistance identification on line, a lot of literature has proposed stator resistance identification programs, which generally can be divided into three categories. One is combined with the measurements of the flux or torque/thrust and the steady-state model motor to calculate the resistance value directly. One is using an adaptive observer to auto identify the resistance on line. One is the use of neural networks, fuzzy control, artificial intelligence techniques to identify the resistance.

Above three methods have each advantages and disadvantages. Because of the larger pulse of the stator current at the low speed, the parameters of conventional PI controller are difficult to determine, which haven't the self-adaptive. The limitation of adaptive estimation is to estimate the amount of value, but only unknown quantity, can't apply to time-varying signal. Identification method based on neural network easy to fall into local optimum, and the algorithm is complex and difficult to achieve.

Combination with the above analysis, if the primary resistance R_s remains constant, the observed value and actual value of the flux are consistent. In fact, the resistance changes with the motor temperature and current frequency. Any resistance variation maybe brings integration error and the actual value of flux does not match with the observed value, which maybe lead to the error choice of the voltage vector and system control performance deterioration [13~15].

B. New Flux Dynamic Compensator Design

The variation of the resistance variation can be seen as the uncertainty of the system from the point of view of the control theory. For the actual uncertainty, whether it is linear, nonlinear, or no matter how complex, one point, which is self-satisfied or changing rate bounded, is basically satisfied. Based on this point, the design of a new flux dynamic compensator is designed, according to the advantages and disadvantages of the PI regulator and the adaptive observer.

The root cause about the inconsistent between the flux observations and the actual value is the resistance changed along with the motor temperature and current frequency in the motor running process, which is unknown process, resulting in the flux deviation from the desired value. In order to clarify the error of the mechanism, the error system will be analyzed firstly.

The ideal value of flux is ψ_s^* in (4) or (5).

$$\begin{aligned} \dot{\psi}_s &= u_s - (R_s + dR_s)(i_s + di_s) \\ &= u_s - R_s i_s - R_s di_s - dR_s \cdot i_s - dR_s \cdot di_s \\ &= u_s - R_s i_s + \mu \end{aligned} \tag{4}$$

$$\psi_s = \int (u_s - R_s i_s + \mu)dt + \psi_{s0} \tag{5}$$

where, $\mu = -R_s di_s - dR_s \cdot i_s - dR_s \cdot di_s$. The i_s is the initial primary current value calculated according to a given flux and thrust value calculated.

The nominal value is defined as in (6).

$$\dot{\psi}_s^* = u_s - R_s i_s \tag{6}$$

In order to achieve the following equation

$$\lim_{t \to \infty} (\psi_s(t) - \psi_s^*(t)) = 0 \tag{7}$$

Equation (4) should be added the compensation *e(t)*, then the following equation is obtained as

$$\dot{\psi}_s = u_s - R_s i_s + \mu + e \tag{8}$$

$$\psi_s = \int (u_s - R_s i_s + \mu + e)dt + \psi_{s0} \tag{9}$$

where, *e(t)* is the additional compensation, whose specific algorithm will be given in the following theorem.

Equation (8) and (6) subtraction gets error equation.

$$\dot{E} = \dot{\psi}_s - \dot{\psi}_s^* = \mu + e \tag{10}$$

In the control system, μ is as the uncertainty of the unknown disturbance, and e can be seen as the control input.

In order to inhibit the effect of the uncertainty μ on flux observer, the following dynamic compensator is structured.

$$\begin{cases}\dot{\xi} = -\lambda\alpha E \\ e = -(\lambda+\alpha)E + \xi\end{cases} \tag{11}$$

From the above analysis, dynamic compensator block diagram is shown in Figure 7.

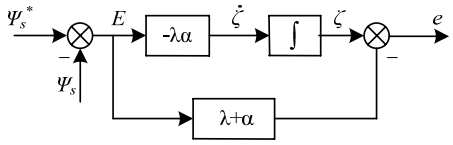

Figure 7. Structure schematic diagram of flux compensator.

C. Compensation Theorem and Proof

Based on the above analysis, the compensation theorem is described as follow.

For (10), there is the dynamic compensator as shown in (11), and the following equation can be got.

$$\lim_{t\to\infty}(\psi_s(t) - \psi_s^*(t)) = 0 \tag{12}$$

The above theorem can be proved. Making $\hat{\mu} = \lambda E - \xi$, from, the following equation can be got.

$$\begin{aligned}\dot{\hat{\mu}} &= \lambda\dot{E} - \dot{\xi} = \lambda(\mu + e) + \lambda\alpha E = \lambda[\mu - (\lambda+\alpha)E + \xi] + \lambda\alpha E \\ &= \lambda[\mu - (\lambda E - \xi)] = \lambda(\mu - \hat{\mu}) = -\lambda(\hat{\mu} - \mu)\end{aligned} \tag{13}$$

$$\dot{\hat{\mu}} - \dot{\mu} = -\lambda(\hat{\mu} - \mu) - \dot{\mu} \tag{14}$$

If $\tilde{\mu} = \mu - \hat{\mu}$, then

$$\dot{\tilde{\mu}} = -\lambda\tilde{\mu} - \dot{\mu} \tag{15}$$

When resistance of the primary winding R_s changes slowly along with the motor temperature increase, the dR_s and di_s are both smaller. So the μ changes slowly and $\dot{\mu} \approx 0$, which can be taken into (15). Then $\dot{\tilde{\mu}} = -\lambda\tilde{\mu}$, and the following equation is got.

$$\lim_{t\to\infty}\tilde{\mu}(t) = \lim_{t\to\infty}\tilde{\mu}(0)e^{-\lambda t} \to 0 \tag{16}$$

When the resistance value R_s changes rapidly, the rate of change is bounded, so the rate of change of μ is bounded. Assuming $\|\dot{\mu}\| \le \rho$, then

$$\tilde{\mu}(t) = \tilde{\mu}(0)e^{-\lambda t} - \int_0^t e^{-\lambda(t-\tau)}\dot{\mu}dt \tag{17}$$

$$\begin{aligned}\|\tilde{\mu}(t)\| &\le \|\tilde{\mu}(0)\|e^{-\lambda t} + \int_0^t e^{-\lambda(t-\tau)}\|\dot{\mu}\|dt \\ &\le \|\tilde{\mu}(0)\|e^{-\lambda t} + \int_0^t e^{-\lambda(t-\tau)}\rho dt \\ &\le \|\tilde{\mu}(0)\|e^{-\lambda t} + \frac{\rho}{\lambda}e^{-\lambda(t-\tau)}\Big|_0^t \\ &\le \|\tilde{\mu}(0)\|e^{-\lambda t} + \frac{\rho}{\lambda} \le \frac{\rho}{\lambda}\end{aligned} \tag{18}$$

Taking $\lambda >> \rho$, then

$$\|\tilde{\mu}(t)\| \le \|\tilde{\mu}(0)\|e^{-\lambda t} + \frac{\rho}{\lambda} \qquad \to \frac{\rho}{\lambda} \approx 0 \tag{19}$$

$$\begin{aligned}\dot{E} &= \mu + e = \mu - (\lambda+\alpha)E + \xi = \mu - (\lambda E - \xi) - \alpha E \\ &= \mu - \hat{\mu} - \alpha E = \tilde{\mu} - \alpha E \approx -\alpha E\end{aligned} \tag{20}$$

Equation (20) can be solved to get the following equation.

$$E(t) = e^{-\alpha t} \tag{21}$$

$$\lim_{t\to\infty}\psi_s(t) = \lim_{t\to\infty}[\psi_s^*(t) + E(t)] = \lim_{t\to\infty}\psi_s^*(t) \tag{22}$$

And then,

$$\dot{E} = \mu - (\lambda+\alpha)E + \xi \tag{23}$$

Even in the face of unexpected factors, the rate of change of μ increases abruptly. But as long as the μ and ξ are both bounded, for $\|\mu + \xi\| \le \rho$ as an example, from (23), the following equation can be got.

$$E(t) = e^{-(\lambda+\alpha)t} + \int_0^t e^{-(\lambda+\alpha)(t-\tau)}(\mu + \xi)d\tau \tag{24}$$

$$\begin{aligned}\|E(t)\| &\le e^{-(\lambda+\alpha)t} + \int_0^t e^{-(\lambda+\alpha)(t-\tau)}\|\mu + \xi\|d\tau \le e^{-(\lambda+\alpha)t} \\ &+ \int_0^t e^{-(\lambda+\alpha)(t-\tau)}\rho d\tau \le e^{-(\lambda+\alpha)t} + \frac{\rho}{\lambda+\alpha} \to \frac{\rho}{\lambda+\alpha}\end{aligned} \tag{25}$$

Taking $\lambda+\alpha >> \rho$, the following equation can be ensured.

$$\|E(t)\| \to \frac{\rho}{\lambda + \alpha} \approx 0 \tag{26}$$

D. Simulation of Compensator Flux Compensation

The simulation model is shown in Figure 8.

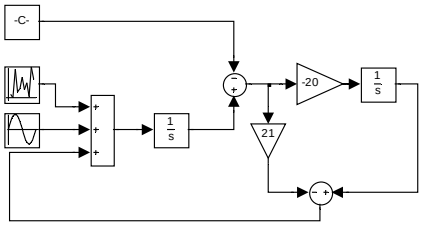

Figure 8. Simulation model of flux linkage compensator performance.

The sine signal is used to as the original e, and the [-0.3, 0.3] random signal is as the interference signal. The given flux is 0.2324Wb. The result is shown in Figure 9.

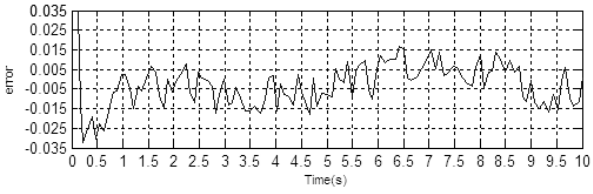

Figure 9. Simulation of dynamic flux linkage compensator.

In the Figure 9, the observation error is within 2% after compensation, having better effect, shown that the compensator is feasible to improve the PMLSM DFC.

The disturbance signal amplification to [-1, 1], again verify the performance of the compensator. Figure 10 shows the error curve.

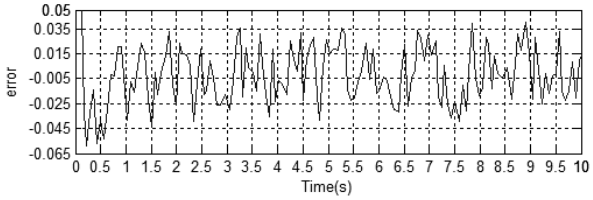

Figure 10. Error curve when interference enlarged.

As Figure 10 shown, the observation error is within 5%. So the compensator shows a very strong robustness.

IV. EXPERIMENT

A. Experimental Platform

Compared with the direct force control (DFC) of hysteresis control, the flux dynamic compensation of SVPWM-DFC, canceled the flux and thrust hysteresis adjustment module and selection module of the switch table and increased the flux dynamic compensator, the primary flux reference vector, the calculation of reference voltage space vector, and the SVPWM module.

The motor control special chip TMS320LF2407A is used as the control core, writing control algorithm. And then the flat car driven testing device of non-salient pole PMLSM was self-developed, in order to test the control performance of the experimental prototype.

The experimental platform of the PMLSM DFC based on SVPWM and flux dynamic compensator is shown in Figure 11.

Figure 11. Experimental platform of the PMLSM DFC.

B. Driven and Control System based on DSP

The driven control system consists of DSP core controller TMS320LF2407A, rectifier filter circuit, inverter, gate drive and protection circuit, detection circuit of the current and voltage, serial communication circuit, encoder signal processing circuit, shown in Figure 12.

The driven part supplies the motor with required power. The control part completes double-loop control with current and speed, and positive and negative control of PMLSM through programming.

Using a common PC, the control algorithm is programmed, and the parameters of the controller is changed, and so on.

The DSP core TMS320LF2407A completes control algorithms. PWM signal is generated by hardware. DSP-driven control system experiment hardware device is shown in Figure 13.

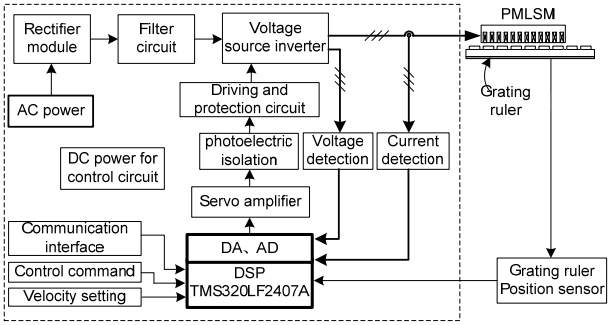

Figure 12. Block diagram of DFC system setup.

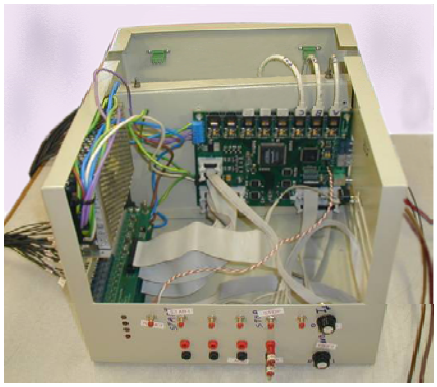

Figure 13. Photograph of DSP drive controller.

C. Experimental Prototype

The Experimental prototype is a self-developed flat PMLSM with long secondary and short primary type. The main technical parameters of the prototype are shown in Table I.

TABLE I.
SPECIFICATIONS OF TEST PMLSM

Parts	Items [units]	Value
Primary	Yoke height [mm]	43
	Pole pitch [mm]	39
	Axial height [mm]	113
Air-gap	Air-gap length [mm]	5
Secondary	PM	NdFeB
	PM height [mm]	7
	PM width [mm]	26

D. Experimental Test System

The hardware of experimental test system mainly includes PC data acquisition device, A/D conversion board, voltage sensor, current sensor, pressure sensor, pulling force sensor, grating ruler, and so on.

Figure 14 shows the block of the test system. Figure 15 shows the computer data acquisition system.

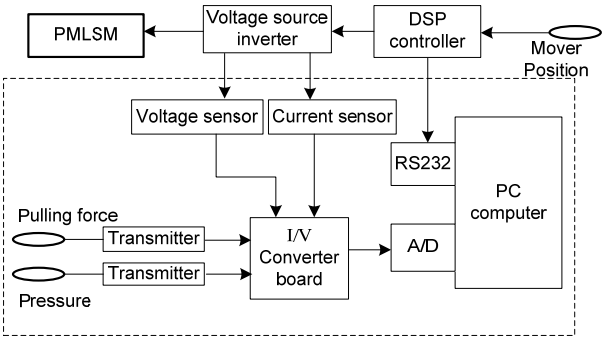

Figure 14. Block of test system.

Figure 15. Computer data acquisition system.

The voltage signals are got through I/V converter board from the several current signals of the sensors. And then the voltage signals are sent to the A/D converter board, which plugged in the PC expansion slot. The A/D high-speed converter board is used to convert the analog channels to the digital conversion, which is collected by PC in the real-time.

E. Testing Set

In the Table II, the initial testing set, the rated load, and maximal load, are shown.

TABLE II.
TESTING SET

Items [units]	Value
Primary flux setting [Wb]	0.2324
Initial load setting [N]	150
Initial speed setting [m/s]	0.312
Rated load [N]	500
Max. load [N]	650

F. Experimental Results

Figure 16 and Figure 17 show the experimental results, including the flux linkage locus waveform, the thrust force waveform, the speed waveform, and A phase current waveform. In Figure 12, the PMLSM starts at the load 150N, and then reduce the load to 100N at 0.8s. In figure 13, the PMLSM starts at the load150N, and then to accelerate at 0.8s.

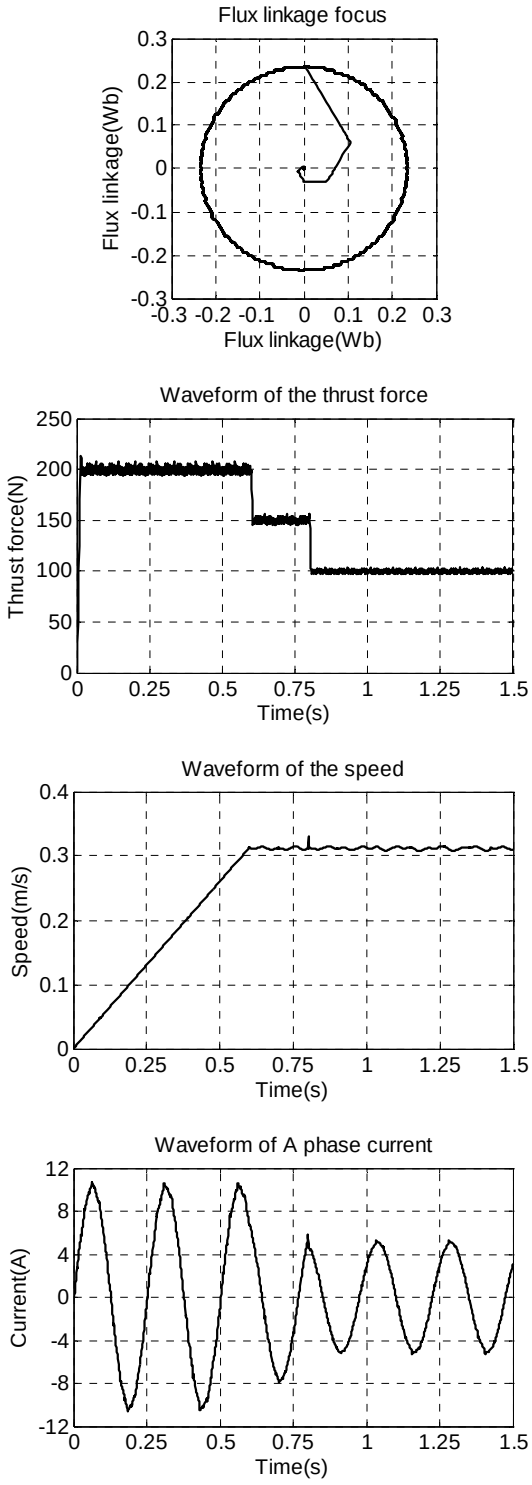

Figure 16. Testing waveforms of the flux-linkage trace, thrust force, speed, and A phase current in the case of load shed to 100N after 150N load starting at 0.8s.

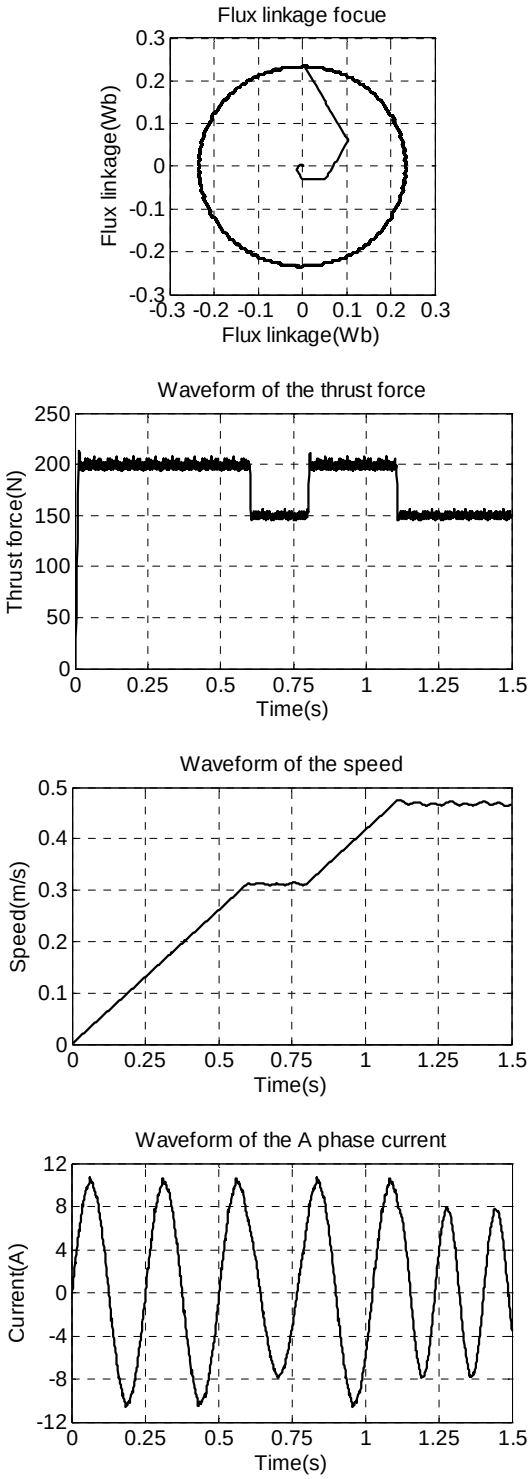

Figure 17. Testing waveforms of the flux-linkage trace, thrust force, speed, and A phase current in the case of accelerate to 0.468m/s after 150N load starting at 0.8s.

As Figure 16 and Figure 17 shown, in the two cases of the PMLSM running process, there is a cyclical fluctuation in the primary flux path, which is similar to the circular. In the PMLSM starting with 150N load, the speed accelerates to the speed setting value 0.312m/s with $0.52m/s^2$ acceleration, corresponding to the Phase A current about 7.54A. After entering the steady-state, the thrust force is almost 150N values in the vicinity of the load fluctuations, corresponding to the A Phase current about 5.66A. Although some fluctuations in speed, but always maintaining a constant. The waveform of the current is approximate the sine.

In the process of load shedding and accelerating, from the point of view on the primary flux linkage locus, thrust variation, speed change, and current trends, the primary flux linkage locus has less fluctuation and closer to the circular. The response of the thrust force is fast and always following the given value. In the speed response curve, the disturbance of speed is obviously smaller when the sudden load reduction. The current curve is similar to the sine. Particularly, the current distortion has been significantly improved when the motor running state changed.

The experimental results show that SVPWM DFC in the PMLSM control based on the flux dynamic compensation is feasible. The flux dynamic compensation algorithm is correctness and useful to improve the dynamic performance of DFC, significantly reducing the fluctuation of the flux and thrust force, further improving the steady-state performance of the PMLSM DFC.

V. CONCLUSION

In this paper, the reasons of the thrust force fluctuation for the conventional PMLSM DFC are analyzed. The SVPWM is introduced into PMLSM control system in order to make the inverter having the continuous voltage vector and reduce the fluctuation of the primary flux and the thrust force. In addition, based on the deeply analysis of flux observer methods, full consideration of the primary winding resistance change during the motor running process, a new flux dynamic compensation algorithm is proposed. Then the primary flux dynamic compensator is designed to improve the accuracy of the flux observation and ensure the accuracy selection of the voltage vector. The experimental results show that the PMLSM DFC based on the SVPWM and flux dynamic compensation, maintains the excellent dynamic performance, and significantly reduces the fluctuation of the flux and the thrust force, shown better control performance.

ACKNOWLEDGMENT

This work was supported by the Foundation for University Key Teacher by Henan Province (2010GGJS-230), and Doctor Foundation of Henan Polytechnic University (2011065), and National Natural Science Foundation of China (NO. 61074095), and Ministry of Education Scientific Research Foundation for Chinese Overseas Returnees and Research Fund for the Doctoral Program of Higher Education (NO. 20104116120001).

REFERENCES

[1] Takahashi, N., Yamada, T., Miyagi, D., “Basic Sudy of Otimal Dsign of Lnear Mtor for Rpe-less Eevator,” *IET 7th International Conference on Computation in Elec-tromagnetics*, n537 CP, 2008, pp. 202-203

[2] Torii, Susumu, Izuno, Naoya, Watada, Masaya, Ebihara, Daiki, “Optimum Cntrol Sheme for the Mximum Eficiency

Dive of Lnear Snchronous Mtor Ued for Rpe-less Eevator," *Electrical Engineering in Japan*, Vol.155, No.3, 2006, pp. 70-78
[3] An Geuk-Sub, Kim Houng-Joong, Ahn Jin-Woo, Koseki Takafumi, "Design and Operating Characteristics of Cylindrical Linear Motor for Long Stroke Precision Stage", *Transactions of the Korean Institute of Electrical Engineers*, Vol. 60, No. 1, 2011, pp. 63-70
[4] Mou Xiaojie, Xu Yuetong, Jiang Fengjun, "Heat Analysis of a Flat Permanent-magnet Linear Synchronous Motor", *Advanced Materials Research*, *Mechatronics and Materials Processing I*, Vol. 328-330, 2011, pp. 974-978
[5] Zhong L, et al., "Analysis of Direct Torque Control in Permanent Magnet Synchronous Motor Drives", *IEEE Transactions on Power Electronics*, Vol. 12, No.3, 1997, pp. 528-536
[6] Yang Junyou, He Guofeng, Cui Jiefan, "Analysis of PMLSM Direct Thrust Control System Based on Sliding Mode Variable Structure", *Conference Proceedings-IPEMC: CES/IEEE 5th International Power Electronics and Motion Control Conference*, Vol.1, 2007, pp. 662-666
[7] Cui Jiefan, "Study on Thrust Force of Permanent Magnet Linear Synchronous Motor and Its Direct Thrust Force Control System", T*hesis and Dissertation Introductions of Shenyang University of Technology*, 2006
[8] W. Hua Gang, X. Wen Li, Y. Gent, "Variable Structure Torque Control of Induction Motors Using Space Vector Modulation", *Electrical Engineering*, No.87, 2005, pp. 93-102
[9] Hong Naigang, "Modeling and Simulation of Power Electronics and Motor Control System", *China Machine Press*, 2010
[10] Zhou Weiping, Wu Zhengguo, Tang Jinsong, Liu Daming, "A Novel Algorithm of SVPWM and the Study on the Essential Relationship Between SVPWM and SPWM", *Proceedings of the CSEE*, Vol.26, No.2, 2006, pp.133-137
[11] Wang Xudong, Feng Haichao, Xu Xiaozhuo, Xu Baoyu, "Modeling and Simulation of Direct Force Control for PMLSM", *Advanced Materials Research*, Vol. 216, 2011, pp. 692-697
[12] Yang Bo, "Sliding Mode Direct Force Control for Linear Drive System", *EPE Journal (European Power Electronics and Drives Journal)*, Vol. 19, No. 1, 2009, pp. 26-32
[13] David L．, Trumper, Won-jong kim，MarkE. Williams, "Design and Analysis Framework for Linear Permanent-Magnet Machines", *IEEE Trans．on Industry Applications*, Vol. 32, No. 2, pp. 371-379
[14] Yang Junyou, Cui Jiefan, He Guofeng, "Direct Thrust control of PMLSM Using SVM and Sliding Model Variable Structure", *Transactions of China Electrotechnical Society*, Vol.22, No.6, 2007, pp. 24-29
[15] Shi Liming, Wang Ke, Li Yaohua, "Direct Thrust Control of Linear Induction Motor Based on Improved Flux Observer", *Transactions of China Electrotechnical Society*, Vol.23, No.9, 2008, pp. 45-50

Haixing Wang was born in China in 1971, and received the PH.D degree in electrical engineering from School of Electrical engineering, China University of Mining and Technology, China, in 2010. His research interests are linear motor theory and application, motor optimization, design of linear motor driving system, energy efficient motors.

He is a professor of Institute of Linear Electric Machines & Drives (LEMD) in Henan Polytechnic University. He accomplished 6 research projects, including the National Natural Science Foundation of China, and over 20 papers was published. He participates in developing many experimental system or products, such as automatic precision servo system, efficient asynchronous motor, self-starting PM motor, and so on.

Dr. WANG is the one of the academic technology leaders, key academic leader of key discipline of Motor and Electrical, and university youth backbone teachers in Henan Province, China.

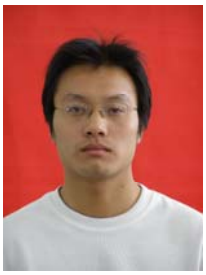

Haichao Feng was born in China in 1983, and received the B.S. and M.S. degrees in electrical engineering and automation, control theory and control engineering from School of Electrical Engineering and Automation, Henan Polytechnic University, china, in 2005 and 2008, respectively. His research interests are the optimization design of linear and rotary machines, power electronics, and their controls.

From 2007 to 2008, he was with ASM Pacific Technology Ltd., HongKong, as a Research Engineer. New, he is a teacher in School of Electrical Engineering and Automation, Henan Polytechnic University, china.

Mr. FENG is a member of institute of linear electric machine and drives, Henan Province, China. In recent years, he participates in 5 provincial and 2 country research projects, published more than 12 academic papers.

Jikai Si was born in Henan Province, China, in 1973. He received the B.S. and M. S. degrees from Jiaozuo Institute and Technology, Henan Polytechnic University, Jiaozuo, China, in 1998 and 2005, respectively. He received the Ph.D. degree in School of Information and Electrical Engineering at China University of Mining and Technology, Xuzhou, China. His main research interests include the theory, application and control of linear motor.

As one of the research term, from 2007 to 2008, he was with ASM Pacific Technology Ltd., HongKong, as a Research Engineer. New, he is a teacher in School of Electrical Engineering and Automation, Henan Polytechnic University, china.

Mr. SI is a member of institute of linear electric machine and drives, Henan Province, China. In recent years, he participates in 8 provincial and 2 country research projects, published more than 30 academic papers.

Nan Wu was born in China in 1980, and received the Bachelor's degree in Eletronic Engineering, and Master's degree in Communication Information system in 2003 and 2009, Zhengzhou University china, respectively. Her research interests include space-time coding for wireless communication system and signal processing for multiple antenna systems.

From 2003 to 2006, she was a teacher in school of Henan Polytechnic University in china.